Journal of Medicinal Chemistry

pubs.acs.org/jmc

Article

Accelerated Identification of Cell Active KRAS Inhibitory Macrocyclic Peptides using Mixture Libraries and Automated Ligand Identification System (ALIS) Technology

Published as part of the Journal of Medicinal Chemistry virtual special issue "New Drug Modalities in Medicinal Chemistry, Pharmacology, and Translational Science".

Michael Garrigou, Bérengère Sauvagnat, Ruchia Duggal, Nicole Boo, Pooja Gopal, Jennifer M. Johnston, Anthony Partridge, Tomi Sawyer, Kaustav Biswas, and Nicolas Boyer*

Cite This: *J. Med. Chem.* 2022, 65, 8961−8974

Read Online

ACCESS | Metrics & More | Article Recommendations | Supporting Information

ABSTRACT: Macrocyclic peptides can disrupt previously intractable protein−protein interactions (PPIs) relevant to oncology targets such as KRAS. Early hits often lack cellular activity and require meticulous improvement of affinity, permeability, and metabolic stability to become viable leads. We have validated the use of the Automated Ligand Identification System (ALIS) to screen oncogenic $KRAS^{G12D}$ (GDP) against mass-encoded mini-libraries of macrocyclic peptides and accelerate our structure−activity relationship (SAR) exploration. These mixture libraries were generated by premixing various unnatural amino acids without the need for the laborious purification of individual peptides. The affinity ranking of the peptide sequences provided SAR-rich data sets that led to the selection of novel potency-enhancing substitutions in our subsequent designs. Additional stability and permeability optimization resulted in the identification of peptide 7 that inhibited pERK activity in a pancreatic cancer cell line. More broadly, this methodology offers an efficient alternative to accelerate the fastidious hit-to-lead optimization of PPI peptide inhibitors.

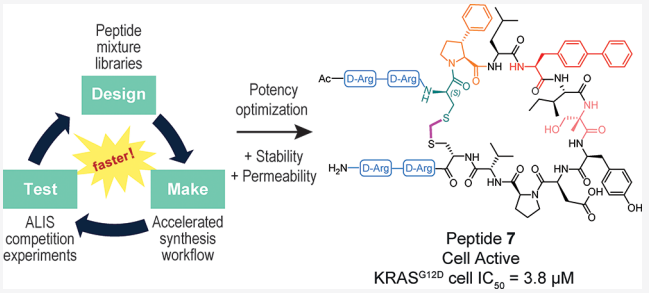

INTRODUCTION

For decades, direct inhibition of the RAS family of oncoproteins has evaded efforts from the drug discovery community. Although the mutated forms of its three isoforms (KRAS, HRAS, and NRAS) account for ∼30% of all human cancers,[1] no pan-RAS therapy has been approved yet. In particular, KRAS represents ∼85% of all mutations and is a major driver of some of the deadliest forms of cancers (pancreatic, colorectal, and lung cancers).[2,3] KRAS was previously deemed "undruggable" owing to its lack of well-defined binding pockets, its inherent flexibility, its various protein−protein interaction partners, and its picomolar affinity for its endogenous ligand, GTP.

The seminal discovery by the Shokat lab of small molecule covalent inhibitors of the mutant $KRAS^{G12C}$,[4] that revealed an unprecedented binding pocket in the switch II region, sparked a surge in research and development activities across industry and academic laboratories.[5,6] Taking advantage of this unique strategy targeting the reactive mutant Cysteine12, novel chemical matter quickly emerged, and several clinical trials were initiated over the past 3 years,[7−10] culminating with the recent U.S. Food and Drug Administration approval of sotorasib (LUMAKRAS). With the promise of treating broader patient populations, other more frequent KRAS mutations such as G12D and G12V are also being investigated, but identifying potent small molecule inhibitors remains a challenging endeavor, despite the recent publication of novel $KRAS^{G12D}$ inhibitors.[11,12] As KRAS signaling pathways function through intracellular PPIs that typically involve large binding surfaces, medicinal chemists have also pursued macromolecular modalities, including nucleic acids, peptides, antibodies, or nonimmunoglobulin proteins.[13,14]

In particular, macrocyclic peptides constitute a modality of growing interest.[15,16] Typically larger (∼500−3000 Da) than conventional small molecules, they are better suited to leverage flat and hydrophobic interfaces characteristic of PPIs and can exhibit antibody-like binding affinity and specificity at a fraction of their molecular weight. Macrocyclic peptides also

Received: February 2, 2022
Published: June 16, 2022

https://doi.org/10.1021/acs.jmedchem.2c00154
J. Med. Chem. 2022, 65, 8961−8974

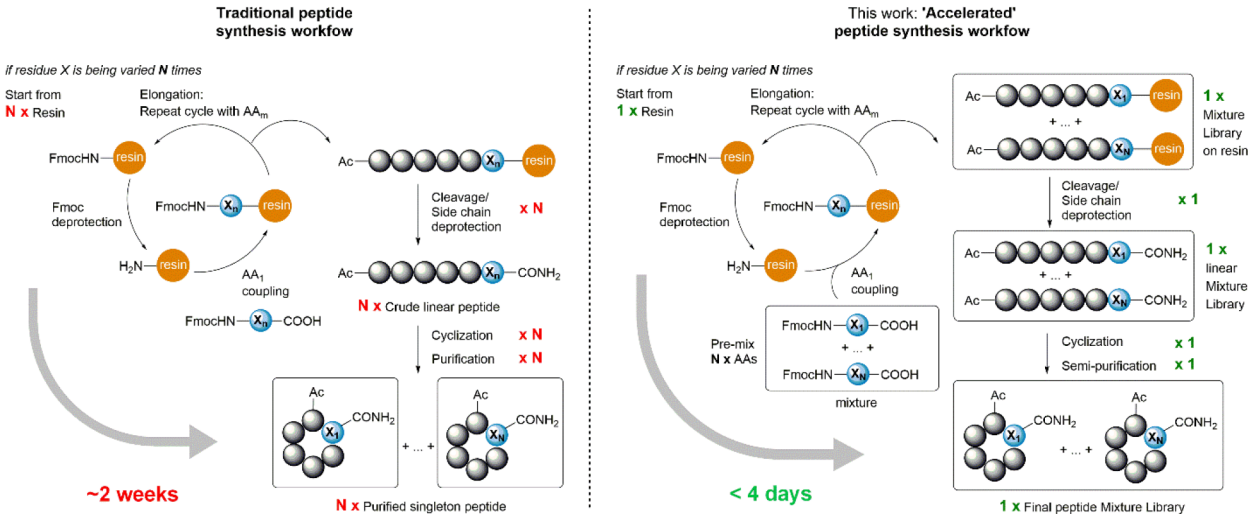

Figure 1. "Accelerated" vs traditional peptide synthesis workflow. For the synthesis of **N** different macrocyclic peptides, the traditional solid-phase peptide synthesis (SPPS) workflow is repeated **N** times, effectively starting from **N** individual solid supports (resins), coupling individual amino acids to build the **N** linear peptides in **N** different containers. Cleavage off the resin, side chain deprotection, and cyclization steps are performed on **N** individual peptides, followed by separate lengthy reversed-phase preparative HPLC purification of the **N** singletons. In contrast, our "accelerated" workflow started from a single standard solid support and involved the coupling of equimolar mixtures of **N** amino acids to the growing peptide to generate the **N** different designed sequences as a mixture in a single container. Upon cleavage and side chain deprotection of the linear peptides off the resin, standard cyclization afforded the crude mixture. Then, a single, fast semipurification using reversed-phase flash column chromatography (FCC) afforded the final mixture library of **N** macrocyclic peptides that was tested in ALIS.

maintain many desirable small molecule properties such as low immunogenic potential and resistance to proteolytic degradation. Emerging from various research groups seeking to take advantage of this modality, several peptidic KRAS inhibitors were recently described.[17−20] In particular, Sakamoto and coworkers reported in 2017 the discovery of a potent macrocyclic peptide inhibitor of KRAS^{G12D} generated by random peptide T7 phage display technology.[21−23] Resulting from the sequence optimization of a phage display screening hit, KRpep-2d (**1**, Figure 2) potently inhibited the SOS1-mediated GDP−GTP exchange. KRpep-2d was also reported to demonstrate high micromolar cellular activity by reducing phosphorylation levels of ERK1/2, a signal transduction pathway downstream of KRAS, and suppressing proliferation of A427 cells containing the KRAS^{G12D} mutation. Despite several desirable properties, the authors concluded that efforts to improve cell membrane permeability resulted in significant cytotoxicity and KRpep-2d efficacy was not sufficient to warrant in vivo studies.

Building from this work and recognizing the potential to address liabilities identified with this peptide, we recently disclosed our discovery of optimized macrocyclic peptide inhibitors based on this scaffold offering multiple improved properties: prolonged metabolic stability, enhanced cell permeability, and validated on-target cellular activity.[24] Our studies substantiated the value of this novel peptide series as an alternate approach toward seeking KRAS-inhibitory chemical matter that could progress the field beyond the recent successes with the KRAS^{G12C} mutant protein. We reported[24] that the KRpep-2d peptide series might inhibit KRAS signaling in at least two distinct ways, by directly blocking the interaction with KRAS effectors (e.g., RAF) as well as by indirectly preventing these interactions by blocking the conversion of the GDP (off) state to the GTP (on) state. Dual inhibition of mutant KRAS signaling is attractive, especially considering the observation that cancer cells can reactivate the MAPK pathway to resist G12C covalent inhibitors, molecules that trap the protein in the GDP state. We also demonstrated that these cell permeable macrocycles were able to inhibit cell growth and block pERK signaling in the low micromolar range in a variety of KRAS^{G12D}, KRAS^{G12C}, and KRAS^{G12V} cancer lines, but not in KRAS^{WT} cell lines, without inducing cytotoxicity (LDH leakage).[24] We also identified off-target challenges inherent in using polyarginine-based cell entry strategies employed by the KRpep-2d chemotype, which contains eight flanking arginine residues. This necessitates continued investment in identifying cell active peptides with reduced arginine burden, which we speculated would require specific modifications to the macrocyclic (non-arginine) core of this peptide. Our initial efforts in that direction are reported in this study.

The use of focused combinatorial libraries is becoming an important weapon in lead exploration and optimization. Various affinity selection-mass spectrometry (AS-MS)-based techniques have been developed over the years to study the interactions of small molecule ligands with their biomolecular targets and identify binders from large pools of compounds such as mixture-based combinatorial libraries.[25−27] The most advanced systems perform the quantitative measurement of K_D's and rank ordering of hits against a protein of interest in solution in an efficient, label-free, and high-throughput manner. In particular, the streamlined Automated Ligand Identification System (ALIS) methodology, an AS-MS platform, fully integrating size exclusion chromatography (SEC) and liquid chromatography (LC)-MS,[28] has successfully been used to discover novel ERK inhibitors,[29] rank order the binding affinities of metabolites in a Factor IXa inhibitor program,[30] enable rapid structure−activity relationship (SAR) around ERK2, MK2, and CHK1 inhibitors when combined with nanoscale synthesis,[31] or even screen RNA targets against small molecule ligands.[32] In contrast, these technologies have not been widely applied to peptide ligand SAR, mainly because

https://doi.org/10.1021/acs.jmedchem.2c00154
J. Med. Chem. 2022, 65, 8961−8974

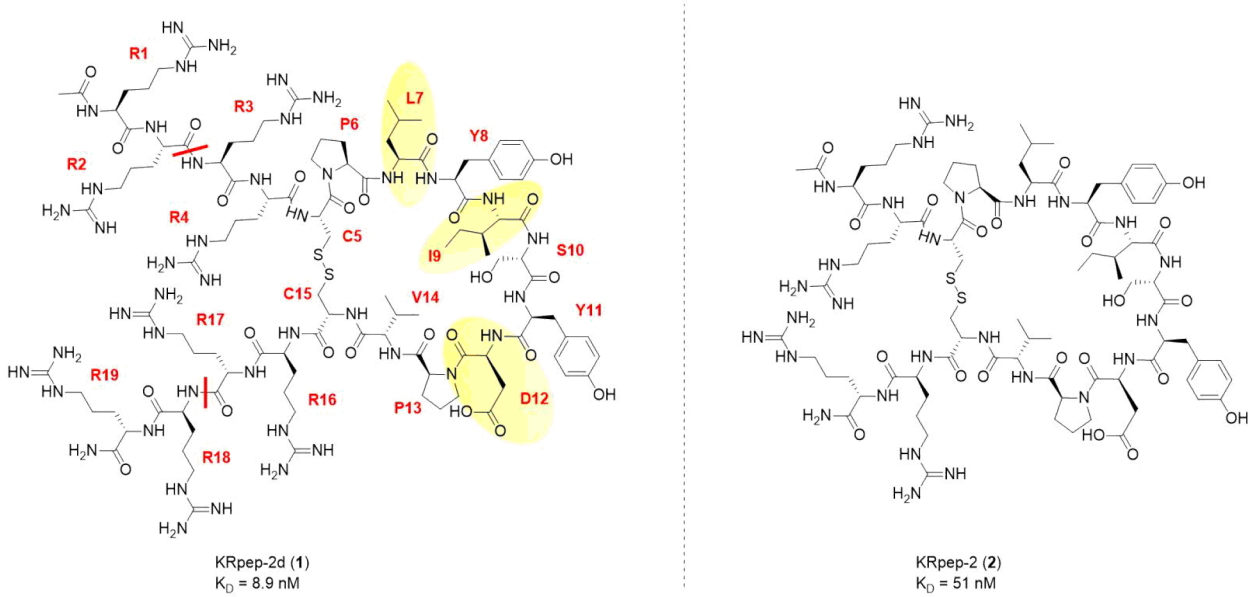

Figure 2. Structures and reported biochemical activities of cyclic peptides KRpep-2d and KRpep-2[21,23] against KRAS^{G12D} (GDP). Standard one-letter codes for canonical amino acids are used to identify residues on KRpep-2d structure. Key binding residues Leu^{7}, Ile^{9}, and Asp^{12} are highlighted in yellow. The only difference between the two structures is the presence of Arg^{1}, Arg^{2}, Arg^{18} and Arg^{19} in KRpep-2d. The same residues numbering was kept for KRpep-2 in this work.

of limitations on MS capabilities to deconvolute complex peptidic mixtures and on synthetic capabilities to generate diverse libraries of peptides. Early work validated the identification of high affinity peptide ligands by screening pools of 19 linear peptides containing canonical amino acids in a solution-phase competition assay.[33,34] More recently, Touti et al. screened large libraries (~10^3–10^6 members) of linear peptides containing non-canonical amino acids using an advanced AS-MS platform similar to ALIS with the objective of identifying peptide inhibitors of PPIs with improved affinity.[35]

Here, we describe how SAR exploration efforts for optimizing a KRAS-inhibitory peptide were accelerated by the implementation of ALIS methodology on mass-encoded libraries of macrocyclic peptides. This process, lessening the need for repeated laborious chromatographic purification methods, expedited the generation of data-rich SAR and resulted in a rapid 50-fold improvement in binding affinity, culminating in the identification and optimization of cell active KRAS^{G12D} inhibitors starting from KRpep-2 (**2**, Figure 2), a KRpep-2d derived scaffold with reduced arginine count that exhibited comparable potency but no cellular activity. This novel chemical matter paves the way in our efforts to identify sequence variants that achieve cell entry without dependence on arginine-rich sequences for achieving in vivo activity against more common KRAS-driven, non-G12C cancers. More broadly, this work exemplifies how a rapid, versatile, and user-friendly affinity selection-mass spectrometry protocol can quickly generate SAR and accelerate the hit-to-lead optimization of PPI peptide inhibitors.

RESULTS AND DISCUSSION

Traditional peptide SAR exploration usually relies extensively on the individual automated solid-phase peptide synthesis (SPPS) of numerous single-point mutated analogues, followed by laborious high-throughput liquid chromatography (HPLC) purification to meet specific purity criteria for testing in relevant biochemical or biophysical assays. To rapidly explore the SAR around the KRpep-2d series of KRAS inhibitors and identify more potent and metabolically stable analogues exhibiting cellular activity with lowered arginine content, we explored alternate SPPS procedures that would provide certain advantages over conventional methods. As such, we sought to validate the screening performance and affinity rank-ordering ability of the ALIS platform on focused libraries of peptide analogues that would be generated via a fast, atom-efficient, "premix" approach.[36,37] This workflow would not require large excesses of costly amino acid building blocks and time-consuming synthesis, postsynthesis workup (e.g., cleavage, precipitation, cyclization), and purification of individual peptides (Figure 1).

To take full advantage of ALIS to not only identify binders within a mixture but also rank-order their relative affinity to the target of interest and generate information-rich SAR to prioritize the next cycle of design, several aspects need to be considered in the context of peptide mixtures. First, the size of a mixture library and the margin in the mass-encoding of individual members can be constrained by the capability of the MS component to detect every binder and deconvolute complex signals (e.g., ion adducts, multiple charge states, etc.). Second, if a library contains compounds with molecular weights that are either too close or identical, additional steps would be required to unambiguously identify the binders. Additionally, without the need for strict stoichiometric control, the synthesis of such a library should at least ensure that all desired peptides are present at comparable concentrations in the mixture (i.e., within one order of magnitude) as the ALIS technology proved to be relatively insensitive to that parameter.[38] Lastly, the parent hit sequence that is being optimized should also be included to the library design as an internal control or reference for the mixture synthesis and subsequent ALIS experiments.

Although our initial objective was to leverage AS-MS to rapidly identify and triage potent analogues of KRpep-2d (**1**),

https://doi.org/10.1021/acs.jmedchem.2c00154
J. Med. Chem. 2022, 65, 8961−8974

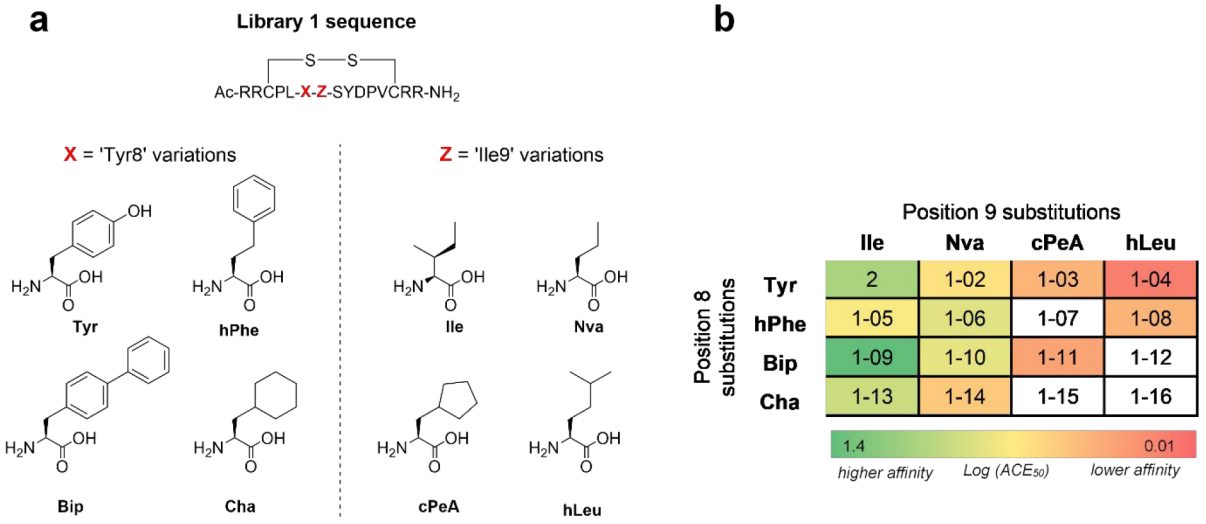

Figure 3. Mixture Library 1 design and ACE_{50} results. (a) Design of premixed amino acids to explore substitutions for Tyr^8 in combination with substitutions for Ile^9. Original Tyr at position 8 and Ile at position 9 were included to serve as internal reference. (b) Peptides were numbered as shown on matrix grid. Heatmap indicates the rank-ordered affinities for $KRAS^{G12D}$ (GDP) measured in ACE_{50} experiment, from red (weaker binders) to green (highest affinity binders). White indicates "not determined".

we quickly realized this experimental strategy would be hampered by several complications. First, its large molecular weight (2561 Da) and the two flanking tetra-arginine appendages on the macrocyclic core represented technical hurdles and synthetic challenges for validating the methodology. Additionally, as we previously reported, KRpep-2d (**1**) exhibited inadequate proteolytic stability and its polycationic character was responsible for off-target effects, namely mast cell degranulation (MCD).[24] Importantly, appropriate retention of arginine-rich analogues on the SEC column of the ALIS system could be compromised and the rate of false positives could be elevated.[32] Such polycationic peptides also tend to behave poorly on LC-MS systems and carry a higher risk of detection issues.

For these reasons, we decided to focus our initial investigation and subsequent validation studies on the closely related analogue KRpep-2 (**2**, Figure 2) from the original publication.[21] This peptide was reported to have comparable biochemical activity and had a reduced count of four arginine residues, thus seeming more technically suitable for ALIS experiments. Published alanine scanning (Ala scan) and structural analysis revealed that Leu^7, Ile^9, and Asp^{12} were key residues for the binding of the macrocycle to $KRAS^{G12D}$ (GDP).[22,23] However, limited side chain optimization to improve potency was reported. Hence, KRpep-2 (**2**) was selected as a reference sequence for our initial library design and an experimental starting point for the validation of the screening of peptide mixtures using ALIS to accelerate the Design−Make−Test cycle and rapidly generate data-rich SAR toward improving its biological activity profile.

Library 1 Design and Synthesis. As a proof of concept for our synthetic methodology, a mixture library of 16 macrocyclic peptide sequences was designed to explore unnatural substitutions in place of Tyr^8 and Ile^9. Metabolite identification studies in cell homogenate suggested that the backbone amide bond was a soft spot for proteolysis in this series.[24] Therefore, we hypothesized that the introduction of unnatural substitutions at these positions could improve the protease stability of the macrocycle. This initial set of combinations was small enough to allow for synthesis optimization but large enough to cover a diverse side chain chemical space as well as explore some potential limitations of the ALIS experiments on macrocyclic peptides. Amino acid building blocks were selected based on four main criteria: (1) relative chemical diversity with respect to the parent natural side chain guided by the published X-ray structure of KRAS-bound KRpep-2d (Figure S1a), (2) mass differentiation, so all designed peptide exact masses were different by at least 1 Da, (3) comparable chemical reactivity toward amide coupling to generate the final pool of peptides at comparable individual concentrations, and (4) building block availability for swift execution of the workflow. With these considerations in mind, we designed our first mini-library to gain some insight on the hydrophobic interactions involving Tyr^8 and Ile^9 residues of the parent scaffold. To interrogate the van der Walls interactions at position 8, we selected substitutions that covered aromatic (L-homophenylalanine, hPhe; L-4,4′-biphenylalanine, Bip) and cycloalkyl moieties (L-cyclohexylalanine, Cha) while the hydrophobic groove occupied by *sec*-butyl side chain of Ile^9 was probed using varied alkyl side chains (L-norvaline, Nva; L-cyclopentylalanine, cPeA; L-homoleucine, hLeu). The original "KRpep-2 combination" of Tyr at position 8 and Ile at position 9 was included in the design of the library to serve as an internal reference in the competition experiments (Figure 3a).

The first key step was the successful construction of the mixture of 16 peptides in *one* routine peptide synthesis experiment. Standard automated SPPS of the linear peptide sequence was performed from a single batch of Rink Amide MBHA resin. The procedure was then modified to couple an equimolar mixture of the designed Fmoc-protected "Tyr^8 variations" and "Ile^9 variations" amino acid building blocks contained in individual reagent vessels attached to the ports for positions 8 and 9, respectively, on the peptide synthesizer. The cleavage and deprotection of the linear peptides using a TFA cocktail followed by precipitation and oxidative formation of the disulfide bridge using a solution of iodine in methanol afforded a crude pool of 16 cyclized peptides in "one pot". A quick "semipurification" using reversed-phase flash chromatography, mostly to remove late-eluting protecting group

https://doi.org/10.1021/acs.jmedchem.2c00154
J. Med. Chem. 2022, 65, 8961−8974

Table 1. Assay Data for Singletons from Library 1

peptide name	sequence	$KRAS^{G12D}$ SOS GNE IC_{50} (nM)	cell homogenate stability (HeLa) $t_{1/2}$ (min)
2 (KRpep-2)	Ac-RR-cyclo(CPLYISYDPVC)-RR-NH_2	54	23
1-02	Ac-RR-cyclo(CPLY-**Nva**-SYDPVC)-RR-NH_2	>11110	19
1-03	Ac-RR-cyclo(CPLY-**cPeA**-SYDPVC)-RR-NH_2	>11110	23
1-04	Ac-RR-cyclo(CPLY-**hLeu**-SYDPVC)-RR-NH_2	>11110	28
1-05	Ac-RR-cyclo(CPL-**hPhe**-ISYDPVC)-RR-NH_2	1387	37
1-06	Ac-RR-cyclo(CPL-**hPhe**-**Nva**-SYDPVC)-RR-NH_2	>11110	15
1-07	Ac-RR-cyclo(CPL-**hPhe**-**cPeA**-SYDPVC)-RR-NH_2	>11110	16
1-08	Ac-RR-cyclo(CPL-**hPhe**-**hLeu**-SYDPVC)-RR-NH_2	>11110	14
1-09	Ac-RR-cyclo(CPL-**Bip**-ISYDPVC)-RR-NH_2	7	55
1-10	Ac-RR-cyclo(CPL-**Bip**-**Nva**-SYDPVC)-RR-NH_2	604	26
1-11	Ac-RR-cyclo(CPL-**Bip**-**cPeA**-SYDPVC)-RR-NH_2	>11110	48
1-12	Ac-RR-cyclo(CPL-**Bip**-**hLeu**-SYDPVC)-RR-NH_2	>11110	17
1-13	Ac-RR-cyclo(CPL-**Cha**-ISYDPVC)-RR-NH_2	161	21
1-14	Ac-RR-cyclo(CPL-**Cha**-**Nva**-SYDPVC)-RR-NH_2	>11110	27
1-15	Ac-RR-cyclo(CPL-**Cha**-**cPeA**-SYDPVC)-RR-NH_2	>11110	21
1-16	Ac-RR-cyclo(CPL-**Cha**-**hLeu**-SYDPVC)-RR-NH_2	>11110	25

remnants, yielded the final mixture library containing the 16 desired macrocyclic peptides at comparable individual concentrations (i.e., within 1 order of magnitude as estimated by UPLC-MS analysis). This was considered acceptable for evaluation of their relative binding affinities for $KRAS^{G12D}$ (GDP) using ALIS.

Library 1 Evaluation in ALIS Experiments. Standard ALIS competition experiments have already been published and extensively reviewed.[28,38] Library 1 was first tested in a protein titration (PT) experiment where the 16 peptides compete for binding to an initial concentration of $KRAS^{G12D}$ (GDP) (Table S7). The competition for binding is then increased by lowering the concentration of the soluble protein in the experiment. At the lowest protein concentration, only the highest affinity compounds remain bound. MS analyses revealed different ranges of affinities for Library 1 peptides, including the presence of several weak binders to nonbinders. More importantly, reference peptide **2** (KRpep-2) and peptide **1-09** appeared to be the best binders in this mixture library.

To obtain a more accurate affinity ranking of the 16 peptides, Library 1 was also tested in an affinity-based competition experiment (ACE), a more labor-intensive experiment that typically relies on the ability of an increasing concentration of a known competitor ligand (titrant) to displace a fixed concentration of protein and mixture of binders, as measured by their MS signals. We selected a close analogue of KRpep-2 as our titrant of comparable affinity (see the Supporting Information (SI)), which allowed the relative binding affinity ranking of the Library 1 peptides (Figure S4). Similar to IC_{50} data obtained from other biochemical competitive assays, the ACE result can be determined for each individual peptide of the mixture as an ACE_{50} value. Of note, a higher affinity for the target is reflected by a higher ACE_{50} value.[30,38] In the case of Library 1, a good agreement with the PT results was observed (Figure S8), gratifyingly indicating that peptide **1-09** (Bip^8/Ile^9) had a higher affinity for $KRAS^{G12D}$ (GDP) than reference peptide **2** (KRpep-2).

When exploring multiple combinations of side chain modifications, ACE_{50} results provide a rich data set where SAR trends can rapidly emerge. The impact on the potency of KRpep-2 can be visualized as a color-coded matrix of the Library 1 ACE_{50} results (Figure 3b). Incorporation of L-4,4′-biphenylalanine (Bip) at position 8 generally appeared to be more favorable than the parent Tyr residue whereas an aliphatic side chain such as Cha proved to be detrimental for binding. At position 9, close aliphatic analogues of Ile at position 9 generally appeared less tolerated, which was consistent with the expected steep SAR for this key residue based on Ala scan data and X-ray structure of KRpep-2d.[22,23]

To validate the affinity rank-ordering of Library 1 sequences generated by the ALIS experiments, we synthesized all 16 peptides individually using standard automated SPPS and tested these singletons (Table 1) in the biochemical SOS-catalyzed guanine nucleotide exchange (GNE) assay that can determine the potency of an inhibitor by its ability to prevent the exchange of a nucleotide Bodipy-GDP-KRAS complex for GTP catalyzed by the guanine nucleotide exchange factor SOS (see the Supporting Information (SI)). Most peptides of this library appeared weak-to-nonbinders in this assay, compared to reference peptide **2** (KRpep-2) with SOS IC_{50} = 54 nM. Gratifyingly, peptide **1-09** (Bip^8/Ile^9) was found to be 8-fold more potent than the reference **2**, which confirmed the beneficial effect of the biaryl side chain at position 8, including in combination with Nva^9 (IC_{50} = 604 nM).

When compared to the results from the ALIS experiments, the SOS data showed a good correlation with PT data (Figure S9), confirming the qualitative ability of this faster and less labor-intensive experiment to quickly distinguish weak-to-nonbinding combinations of substitutions from the desired higher-binding ones that can be explored further in the next design cycle. More strikingly, we observed an excellent correlation with the ACE_{50} data (Figure 4) for peptides with submicromolar potencies, highlighting the accurate rank-ordering of the peptides in our Mixture Library 1 and the improved potency of peptide **1-09** over reference peptide **2** (KRpep-2).

Despite the presence of unnatural side chains at positions 8 and 9, the half-life of these singletons in our HeLa cells homogenate stability assay (see the SI for details) was found to be very modest and comparable to that of the reference **2** (KRpep-2, $t_{1/2}$ = 23 min), suggesting that additional structural modifications might be necessary to mitigate their metabolic liability. We had also demonstrated that the redox-sensitive disulfide cyclization motif of these macrocycles was a barrier to achieving cellular activity but that this issue could be addressed by disulfide replacement with a linkage that preserved binding

https://doi.org/10.1021/acs.jmedchem.2c00154
J. Med. Chem. 2022, 65, 8961−8974

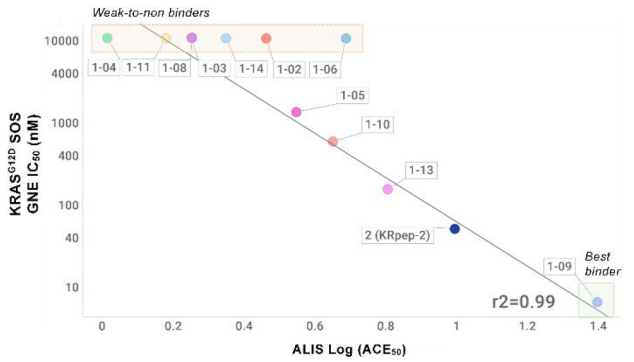

Figure 4. Correlation of SOS potencies for Library 1 singletons against ACE_{50} results for Mixture Library 1. Regression was performed on peptides binding in both the ACE and SOS assay. Peptide **1-09** emerged as the best binder of the library, with an 8-fold improvement in SOS potency over KRpep-2 (**2**).

affinity.[24] We applied changes to our new analogues to improve overall proteolytic/redox stability after completion of multiple rounds of ALIS-based potency optimization (vide infra).

Recognizing the potential of the ALIS methodology to quickly improve the potency of our peptides while building extensive SAR, we designed a second mixture library aiming to explore new unnatural substitutions at the positions 10 and 11 of KRpep-2 that appeared, from the published Ala scan,[22] amenable to modification and potential potency gain.

Library 2 Design and Synthesis. Next, we applied the same principles as for Library 1 to generate Ser^{10} and Tyr^{11} variations (Figure 5a) suitable for ALIS experiments and covering a diverse chemical space guided by the KRpep-2d X-ray structure (Figure S1b). For position 10, we sought to interrogate the H-bond between Ser^{10} and Asp^{69} of KRAS by either incorporating a charged side chain (L-2,4-diaminobutyric acid, Dab), abrogating the H-bond donor/acceptor (L-norleucine, Nle), or introducing a thiazole, a noncharged heterocyclic H-bond acceptor side chain (L-4-thiazolylalanine, Tza). For position 11, we explored larger aromatic (L-diphenylalanine, Dip; 3,4,5-trifuoro-L-phenylalanine, Phe345F3) or cycloalkyl (Cha) side chains for the hydrophobic pocket occupied by Tyr^{11}. Mixture Library 2 was synthesized from a single resin using the accelerated aforementioned workflow and made available for ALIS testing in under 4 days.

Library 2 Evaluation in ALIS Experiments. We tested the Mixture Library 2 in a PT experiment that revealed the presence of peptides covering a wide range of affinities for $KRAS^{G12D}$, including the best binders **2-02** and **2-03** showing the same level of affinity as the reference sequence **2** (KRpep-2) (Table S8). However, the evaluation of Library 2 in the ACE experiment showed a better potency of the reference **2** over peptides **2-02** and **2-03** (Figure S5). Interestingly, the limited SAR around Ser^{10} appeared fairly restrictive compared to Tyr^{11} that seemed more tolerant toward different aromatic side chains (Figure 5b).

To increase confidence in our methodology, we selected half of Library 2 peptides covering a wide range of affinities and resynthesized them as singletons. Upon testing in the SOS assay (Table 2), no peptide was found to have better affinity than the reference **2** (KRpep-2, IC_{50} = 54 nM) and peptide **2-03** was the second-best binder of this library with an IC_{50} of 193 nM.

Nevertheless, these results correlated again very well with the PT (Figure S11) and ACE_{50} results (Figure 6) which demonstrated the ability of ALIS competition experiments to quickly identify weak-to-nonbinders as well as potent binders from Mixture Library 2, and rank-order their KRAS affinities.

After the validation of our methodology in a first round of designs based on KRpep-2 sequence, we sought to further improve the potency of peptide **1-09** that emerged as the best binder to KRAS from Libraries 1 and 2. We also sought to expand the SAR around given positions by increasing the number of premixed amino acids in our libraries.

Libraries 3 and 4 Design and Synthesis. To pursue the combinatorial SAR exploration of other key residues of our macrocyclic KRAS inhibitors, we designed Mixture Library 3 with varied side chains at positions 6 and 7 for a total of 28 different combinations (Figure 7a). Structural and modeling information (Figure S1c) indicated a potential to improve the interaction with the protein (nearby groove residues Asp^{92}, His^{95}, Tyr^{96}) via a substitution on Pro^{6} and to benefit from the stabilization of the proline conformation. We chose a

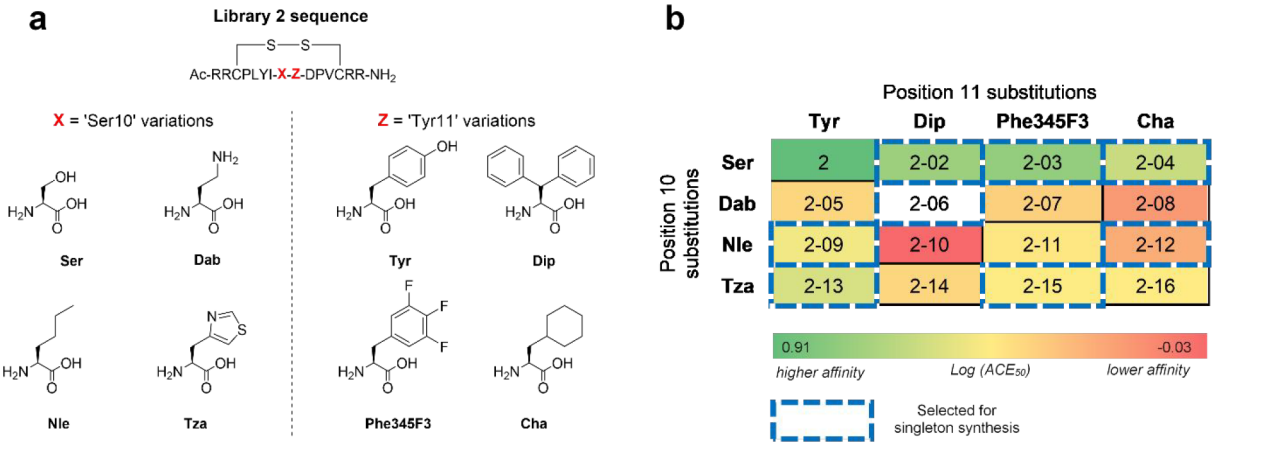

Figure 5. Mixture Library 2 design and ACE_{50} results. (a) Design of premixed amino acids to explore substitutions for Ser^{10} in combination with substitutions for Tyr^{11}. Original Ser at position 10 and Tyr at position 11 were included to serve as internal references. (b) Peptides were numbered as shown on the matrix grid. Heatmap indicates the rank-ordered affinities for $KRAS^{G12D}$ (GDP) measured in the ACE_{50} experiment, from red (weaker binders) to green (highest affinity binders). White indicates "not determined".

https://doi.org/10.1021/acs.jmedchem.2c00154
J. Med. Chem. 2022, 65, 8961−8974

Table 2. Data for Selected Singletons from Library 2[a]

peptide name	sequence	KRAS^{G12D} SOS GNE IC_{50}(nM)	cell homogenate stability (HeLa) $t_{1/2}$ (min)
2 (KRpep-2)	Ac-RR-cyclo(CPLYISYDPVC)-RR-NH_2	54	23
2-02	Ac-RR-cyclo(CPLYIS-**Dip**-DPVC)-RR-NH_2	251	30
2-03	Ac-RR-cyclo(CPLYIS-**Phe345F3**-DPVC)-RR-NH_2	193	18
2-04	Ac-RR-cyclo(CPLYIS-**Cha**-DPVC)-RR-NH_2	1474	15
2-06	Ac-RR-cyclo(CPLYI-**Dab**-**Dip**-DPVC)-RR-NH_2	>11110	34
2-09	Ac-RR-cyclo(CPLYI-**Nle**-YDPVC)-RR-NH_2	>11110	25
2-12	Ac-RR-cyclo(CPLYI-**Nle**-**Cha**-DPVC)-RR-NH_2	>11110	26
2-13	Ac-RR-cyclo(CPLYI-**Tza**-YDPVC)-RR-NH_2	2269	22
2-15	Ac-RR-cyclo(CPLYI-**Tza**-**Phe345F3**-DPVC)-RR-NH_2	>11110	ND

[a]ND = Not determined.

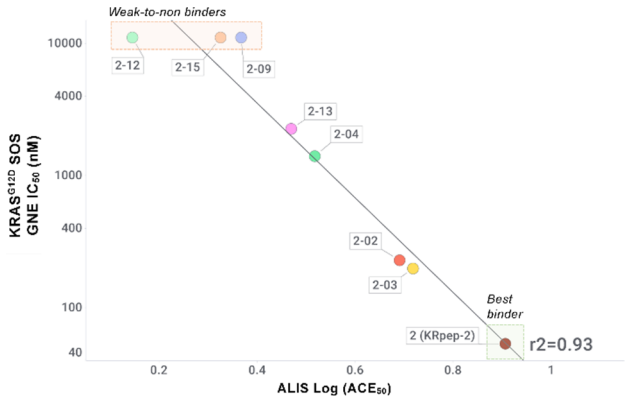

Figure 6. Correlation of SOS potencies for Library 2 singletons against ACE_{50} results for Mixture Library 2. Regression was performed on peptides binding both in ACE and SOS assay. No peptide showed improved potency over reference **2** (KRpep-2).

structurally diverse set of neutral or charged moieties (*trans*-3-allyloxy-L-proline, Prot3OAl; *cis*-4-fluoro-L-proline, Proc4F; *trans*-4-(carboxymethoxy)-L-proline, Prot4OAcOH) as well as cyclic aromatics (*trans*-3-phenyl-L-proline, Prot3Ph) or saturated groups (*cis*-3,5-cyclopentyl-L-proline, sProc35c2; *trans*-4-cyclohexyl-L-proline, Prot4cHex), covering various positions and orientations to interrogate different vectors off the pyrrolidine ring of Pro[6]. For position 7, we adopted related cyclic (L-cyclobutylalanine, Cba; Cha) or acyclic polar (*O*-methyl-L-serine, SerOMe) aliphatic analogues of Leu, anticipating a tight SAR around this key binding residue buried in a hydrophobic pocket.

Library 4 (Figure 7b) included chemical diversity around two solvent exposed residues, Pro[13] and Val[14] (Figure S1d). Although no additional intermolecular interaction with KRAS was expected from Pro[13] analogues, we hypothesized that substituents off the pyrrolidine ring could potentially affect the conformation of the proline and consequently the bioactive conformation of the macrocycle. Similarly, a diverse set of substitutions at position 14 was anticipated to modify the binding of the macrocycle through conformational effect in addition to its reported interaction with Arg[102] via van der Waals stacking.[23]

Both mixture libraries integrated these modifications to the improved reference scaffold of peptide **1-09** containing Bip[8] and were rapidly synthesized following our accelerated workflow.

Libraries 3 and 4 Evaluation in ALIS Experiments. The PT experiment on Mixture Library 3 quickly indicated that combinations **3-05**, **3-07**, **3-09**, and reference **1-09** had the

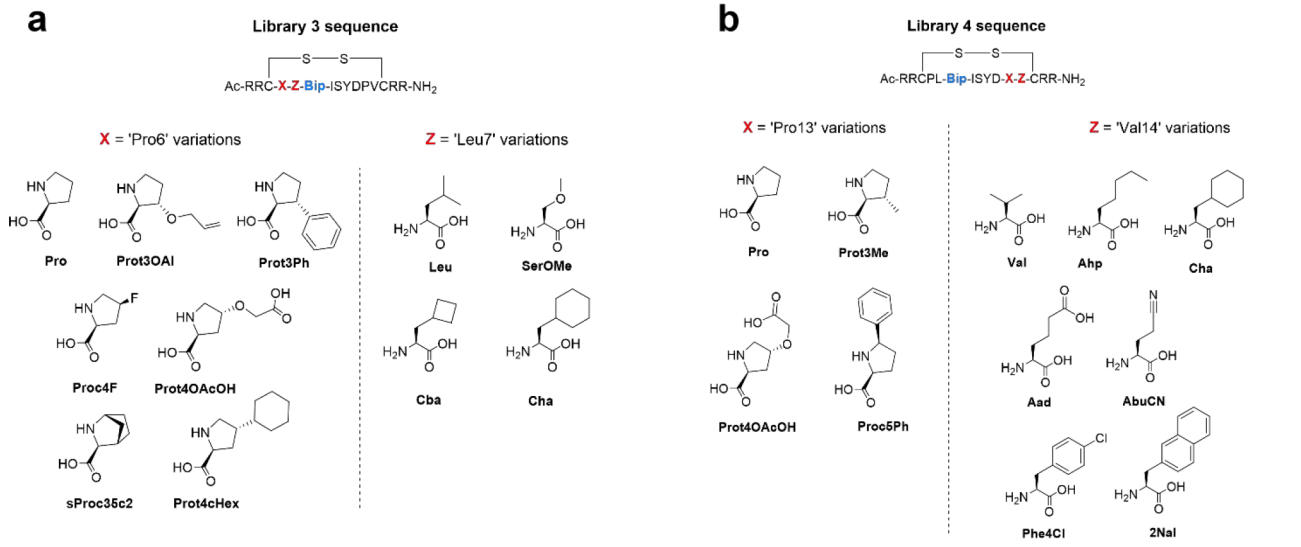

Figure 7. Mixture Libraries 3 and 4 design. (a) Design of premixed amino acids to explore substitutions for Pro[6] in combination with substitutions for Leu[7]. Original Pro at position 6 and Leu at position 7 were included to serve as internal reference. (b) Design of premixed amino acids to explore substitutions for Pro[13] in combination with substitutions for Val[14]. Original Pro at position 13 and Val at position 14 were included to serve as internal reference.

https://doi.org/10.1021/acs.jmedchem.2c00154
J. Med. Chem. 2022, 65, 8961−8974

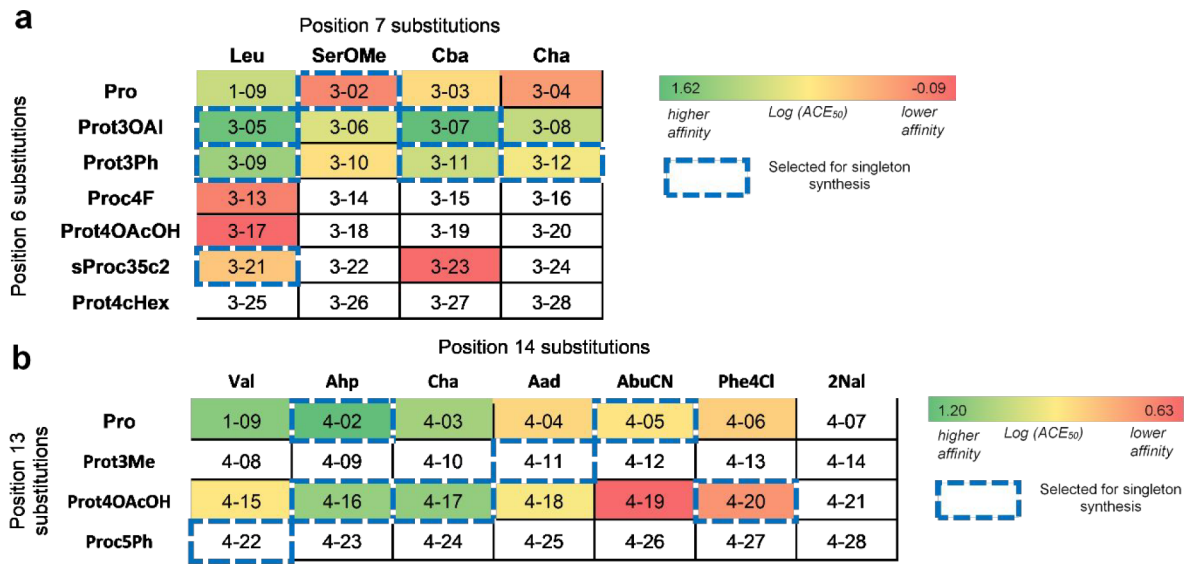

Figure 8. Mixture Libraries 3 (a) and 4 (b) ACE_{50} results. Peptides were numbered as shown on the matrix grid. Heatmap indicates the rank-ordered affinities for KRAS measured in ACE_{50} experiment, from red (weaker binders) to green (highest affinity binders). White indicates "not determined".

Table 3. Data for Selected Singletons from Libraries 3 and 4

peptide name	sequence	$KRAS^{G12D}$ SOS GNE IC_{50} (nM)
1-09	Ac-RR-cyclo(CPL-**Bip**-ISYDPVC)-RR-NH_2	7
3-02	Ac-RR-cyclo(CP-**SerOMe**-**Bip**-ISYDPVC)-RR-NH_2	1133
3-05	Ac-RR-cyclo(C-**Prot3OAl**-L-**Bip**-ISYDPVC)-RR-NH_2	1
3-07	Ac-RR-cyclo(C-**Prot3OAl**-**Cba**-**Bip**-ISYDPVC)-RR-NH_2	2
3-09	Ac-RR-cyclo(C-**Prot3Ph**-L-**Bip**-ISYDPVC)-RR-NH_2	1
3-11	Ac-RR-cyclo(C-**Prot3Ph**-**Cba**-**Bip**-ISYDPVC)-RR-NH_2	7
3-12	Ac-RR-cyclo(C-**Prot3Ph**-**Cha**-**Bip**-ISYDPVC)-RR-NH_2	20
3-21	Ac-RR-cyclo(C-**sProc35c2**-L-**Bip**-ISYDPVC)-RR-NH_2	201
4-02	Ac-RR-cyclo(CPL-**Bip**-ISYDP-**Ahp**-C)-RR-NH_2	5
4-05	Ac-RR-cyclo(CPL-**Bip**-ISYDP-**AbuCN**-C)-RR-NH_2	24
4-11	Ac-RR-cyclo(CPL-**Bip**-ISYD-**Prot3Me**-**Aad**-C)-RR-NH_2	43
4-16	Ac-RR-cyclo(CPL-**Bip**-ISYD-**Prot4OAcOH**-**Ahp**-C)-RR-NH_2	23
4-17	Ac-RR-cyclo(CPL-**Bip**-ISYD-**Prot4OAcOH**-**Cha**-C)-RR-NH_2	25
4-20	Ac-RR-cyclo(CPL-**Bip**-ISYD-**Prot4OAcOH**-**Phe4Cl**-C)-RR-NH_2	33
4-22	Ac-RR-cyclo(CPL-**Bip**-ISYD-**Proc5Ph**-VC)-RR-NH_2	94

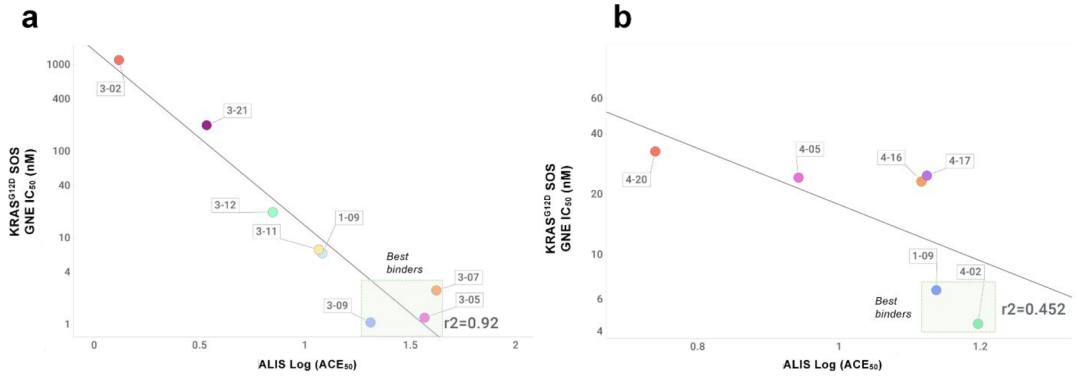

Figure 9. Correlation of SOS potencies for Libraries 3 (a) and 4 (b) singletons against ACE_{50} results. Regression was performed on peptides binding both in ACE and SOS assays. Peptides **3-05**, **3-07**, **3-09**, and **4-02** showed improved potency over reference **1-09**.

best affinity for KRAS (Table S9). This was further confirmed by the ACE_{50} measurements that showed an increased potency for peptides **3-05**, **3-07**, and **3-09** compared to reference **1-09** (Figure S6). In addition, the color-coded matrix of ACE_{50} values (Figure 8a) clearly highlighted that the *trans* vector at position 3 of the pyrrolidine ring of Pro^6 seemed much more tolerated than all other substituents tested. Substitutions at position 4 as well as bridged bicyclic systems were not

https://doi.org/10.1021/acs.jmedchem.2c00154
J. Med. Chem. 2022, 65, 8961−8974

Table 4. Data for Cell Active Combination Peptides

peptide name	sequence[a]	$KRAS^{G12D}$ SOS GNE IC_{50} (nM)	AlphaScreen (AsPC-1) 2 h IC_{50} (μM)	AlphaScreen (AsPC-1) 18 h IC_{50} (μM)	cell homogenate stability (HeLa) $t_{1/2}$ (min)
5-01	Ac-RR-cyclo(**c(methylene)-Prot3Ph**-L-**Bip**-ISYDPVC)-RR-NH_2	<1	3.3	33	>372
5-02	Ac-RR-cyclo(**c(methylene)-Prot3OAl**-L-**Bip**-ISYDPVC)-RR-NH_2	<1	28	>50	260
5-03	Ac-RR-cyclo(**c(methylene)-Prot3Ph**-L-**Bip**-ISYDP-**Ahp**-C)-RR-NH_2	<1	6.8	29	>372
5-04	Ac-RR-cyclo(**c(methylene)-Prot3OAl**-L-**Bip**-ISYDP-**Ahp**-C)-RR-NH_2	<1	30	>50	ND

[a]Lowercase letters represent D-amino acids. ND = Not determined.

tolerated. Results on variations of the conserved residue Leu^7 indicated only a comparable level of affinity for the most structurally similar Cba and to a lesser extent Cha.

We also performed both ALIS competition experiments on Mixture Library 4 (Table S10, Figure S7) that highlighted a potential improvement of potency only for peptide **4-02**. SAR trends derived from the ACE_{50} matrix (Figure 8b) showed a detrimental effect of the substituents placed at positions 3 and 5 of the 5-membered ring of Pro^{13} while Prot4OAcOH with a substituent at position 4-*trans* was moderately tolerated. The impact of varying residues at Val^{14} seemed generally less critical although extended or cyclic aliphatic analogues (L-2-aminoheptanoic acid, Ahp; Cha) as well as the charged L-α-aminoadipic acid (Aad) seemed to maintain affinity. Large aromatics were detrimental to binding.

Next, we sought to further leverage the predictive power of the ALIS competition experiments to optimize a hit sequence and generate data-rich SAR, demonstrated with Mixture Libraries 1 and 2 by reducing the number of individual peptides that needed singleton synthesis and purification. We selected only the best binders in each library as well as a few additional combinations predicted to be weak binders for resynthesis and testing in the SOS assay (Table 3).

For the selected peptides of Library 3, we were pleased to observe an excellent correlation with ACE results over a wide range of affinities (Figure 9a). Peptides **3-05** and **3-09** showed the best potency against KRAS with both having an IC_{50} of 1 nM, a 7-fold improvement over reference peptide **1-09** (IC_{50} = 7 nM). These results confirmed the beneficial effect of a *trans* substituent at position 3 of Pro^6.

Upon testing of selected Library 4 singletons, only a moderate correlation with ACE results was observed (Figure 9b), which could be attributed to an unexpected effect of the charged proline substituent in Prot4OAcOH. Nevertheless, peptide **4-02** was confirmed to be similar in potency (IC_{50} = 5 nM) than reference peptide **1-09**.

Overall, from these two rounds of optimization of KRpep-2 using mixture libraries in ALIS experiments, several KRAS peptide inhibitors successfully emerged with a low single-digit nanomolar potency (a 50-fold improvement in binding affinity) and a diverse SAR on the peptide macrocycle side chains was rapidly generated.

Further Optimization Toward Cellular Activity. Although we were able to substantially increase the KRAS binding affinity of the parent scaffold with the beneficial modifications identified in this study, these peptides were not able to functionally block cellular KRAS activity as measured by their impact on downstream signaling in an AlphaScreen pERK assay in AsPC-1 cells, a pancreatic cancer line homozygous for $KRAS^{G12D}$.[24] We hypothesized that our optimized peptides still suffered from the inherent redox instability of their disulfide bridge in the intracellular reducing environment and from poor proteolytic stability (HeLa homogenate $t_{1/2}$ of peptide **3-09** = 14 min), likely impacting cellular activity. To address these issues, we first considered two key modifications we identified previously[24] that impart redox stability while maintaining a nearly identical peptide conformation in the bound state: (1) the inversion of chirality at position 5 (Cys^5 → D-Cys) and (2) the insertion of a reduction-resistant methylene bridge between the two cysteines of the macrocycle. Combining these elements with the best mutations identified by ALIS (i.e., peptides **3-05**, **3-09**, and **4-02**), we synthesized four combination peptides and evaluated them for their ability to inhibit KRAS signaling pathways in AsPC-1 cells (Table 4).

We were pleased to observe that the combination of the stable D-Cys^5−methylene−Cys^{15} linkage with the mutations of key residues within the macrocycle resulted in subnanomolar SOS GNE potency as well as increased stability in our cell homogenate assay with half-lives ranging from 260 to >372 min. Gratifyingly, the incorporation of these optimized substitutions provided our first cell active macrocyclic peptides containing only four arginines and inhibiting pERK activity, with peptide **5-01** exhibiting an IC_{50} of 3.3 μM at the 2 h time point. As noted previously, macrocyclic peptides with mixed apolar/cationic character have a high propensity for false positives in cellular assays, prompting the need for routine counter screens. The analogues in this series appeared to be on-target as they did not affect the integrity of the membrane (as measured by an 18 h LDH release assay) and were inactive in a counter screen in A375 cells, a RAS-independent cell line harboring $BRAF^{V600E}$, a MAPK pathway activating mutation downstream of KRAS (Table S11).

We modeled peptide **5-01** (Table 4) in the binding site of $KRAS^{G12D}$ in complex with GMPPCP using MOE.[39] Beginning from a minimized complex (PDB ID: 7ROV),[24] the in silico modifications to make peptide **5-01** were made manually. This modified structure was then further minimized, and we carried out local conformational searching of the peptide around $Prot3Ph^6$, Arg^3, and Leu^7, using the MOE Low Modes MD routine, to sample the possible orientations of the phenyl ring in the receptor pocket, which was held fixed. A selection of three of the most diverse of the conformations was further minimized within a flexible receptor (Figure S16). Variation in the side chain of Arg^3 and a change in the pucker of the pyrrolidine ring of $Prot3Ph^6$ can orient the phenyl substituent toward stacking against the His^{95} side chain. The Bip side chain at position 8 presents extended surface area compared to the original Tyrosine, enhancing van der Waals interactions with the Tyr^{64} from the Switch II loop of KRAS.

https://doi.org/10.1021/acs.jmedchem.2c00154
J. Med. Chem. 2022, 65, 8961−8974

Table 5. Potency, Stability, and Permeability Data of Optimized Cell Active Peptides

peptide name	sequence[a]	KRAS^{G12D} SOS GNE IC_{50} (nM)	AlphaScreen (AsPC-1) 2 h IC_{50} (μM)	AlphaScreen (AsPC-1) 18 h IC_{50} (μM)	cell homogenate stability (HeLa) $t_{1/2}$ (min)	NanoClick (HeLa) 4 h EC_{50} (nM)	NanoClick (HeLa) 18 h EC_{50} (nM)
6	Ac-**Lys(N_3)**-RR-cyclo(**c(methylene)-Prot3Ph**-L-**Bip**-ISYDPVC)-RR-NH_2	<1	2.7	19	>372	7316	199
7	Ac-**rr**-cyclo(**c(methylene)-Prot3Ph**-L-**Bip**-I-**aMeS**-YDPVC)-**rr**-NH_2	<1	3.8	3.9	>372	n/a	n/a
9	Ac-**Lys(N_3)-rr**-cyclo(**c(methylene)-Prot3Ph**-L-**Bip**-I-**aMeS**-YDPVC)-**rr**-NH_2	<1	6.2	6.8	>372	1488	148

[a]Lowercase letters represent D-amino acids. n/a = not applicable. See the SI for data related to cell inactive peptides **8** (Table S12) and **10** (Table S13).

Next, we sought to confirm the cell permeability of our analogues. Previously, we showed that a reduced number of arginines compared to the parent KRpep-2d (**1**) architecture was detrimental to cellular uptake mechanisms.[24] Cellular permeability was assessed using our cell-based NanoClick assay that relies on the "Click" reactivity of azide-containing peptides to measure their accumulation in the cytosol.[40] We synthesized the corresponding "azido-analogue" of peptide **5-01**, peptide **6**, containing an azido-lysine at the *N*-terminus and compared it with permeable and impermeable controls (Table S13). Also tested in the SOS GNE and AlphaScreen assays, peptide **6** showed subnanomolar SOS assay potency and pERK IC_{50} = 2.7 μM (Table 5), confirming that the azido-tag was only minimally altering the properties of peptide **5-01**.

Interestingly, peptide **6** showed limited permeability after 4 h but a much-increased permeability at 18 h, despite exhibiting a 6-fold improved cellular activity at 2 h versus 18 h. Since permeability was not the only parameter impacting cell activity, this difference might be attributed to the difference in uptake efficiency of the two cell lines (HeLa vs AsPC-1) but also to the decreasing stability of the peptide over time that would not be compensated by increased permeability.

Finally, we integrated specific additional modifications previously identified[24] as beneficial for the proteolytic stability of this scaffold: (1) replacement of canonical L-arginines by their enantiomeric counterparts (Arg → D-Arg) and (2) introduction of α-methylation at position 10 (Ser^{10} → α-methyl-L-serine). Gratifyingly, the resulting peptide **7** (Table 5) maintained a subnanomolar potency and exhibited a sustained cellular activity (IC_{50} (2 h) = 3.8 μM, IC_{50} (18 h) = 3.9 μM), with no LDH release or activity in our A375 cells counter-screen assay (Table S11). Its on-target cellular activity was further validated with a nonbinding control peptide **8**, where the only modification was that the key macrocycle residue Ile^9 was replaced for its enantiomeric counterpart (D-Ile) to maintain the overall chemical composition, that showed no response in the SOS assay as well as no cellular activity (Table S12).

We also confirmed its permeability by testing its "azido-analogue", peptide **9**, in our NanoClick assay. Compared to peptide **6**, we observed an improved permeability at 4 h (EC_{50} = 1.5 μM) and a maintained excellent permeability at 18 h (EC_{50} = 0.15 μM). Interestingly, we found that the close analogue peptide **10**, with the "parent" macrocycle residues, and not carrying the beneficial side chains identified in this study at positions 6, 8, and 10, showed no permeability at 4 h and very limited permeability at 18 h (Table S13), which could be attributed to their difference in lipophilicity ($ALogP_{98}$ peptide **9** = −3.3; $ALogP_{98}$ peptide **10** = −6.7). This data suggested that this much-improved permeability, contributing to peptide **9** and, by extension, peptide **7** cellular activities, concurrently emerged from our optimization and incorporation of specific lipophilic residues in the peptide macrocycle.

These studies therefore accomplished a couple of objectives that we were seeking. First, we were able to execute on establishing an accelerated peptide synthesis−testing workflow in the laboratory, improving the turnaround cycle time between peptide design and in vitro assay data generation, using ALIS as a comparative affinity evaluation tool. Second, the potency-impacting core macrocycle modifications that were uncovered in this process led to the identification of cell active KRAS inhibitors with a reduced arginine count compared to the bis(tetra-arginine)-containing KRpep-2d (**1**). As we have shown previously, high arginine content is correlated to mast cell degranulation-related liabilities, preventing further progression of this series.[24] Contrarily, we observed the elimination of cell activity upon arginine truncation of the parent macrocycle. Therefore, our current SAR observations combine arginine truncation with targeted lipophilic modifications of the core macrocycle to *restore* the cellular activity of the parent bis(tetra-arginine) system, providing design strategies toward eventual access to cell active KRAS-binding peptides without cationic cell-penetrating segment motifs.

CONCLUSION

Herein we demonstrated that the ALIS technology could be employed to screen KRAS^{G12D} (GDP) against focused mixture libraries of macrocyclic peptide inhibitors and to rapidly evolve the initial hit KRpep-2 toward subnanomolar binders. The affinity-ranking of our designed sequences generated by ALIS competition experiments enabled the identification of novel beneficial mutations of the KRpep-2 macrocycle, including *trans*-3-phenyl-L-proline at position 6 and L-4,4′-biphenylalanine at position 8, that represented a combined >50-fold enhancement in potency in biochemical assays.

More generally, we believe this methodology can accelerate the generation of useful SAR around a macrocyclic peptide hit to rapidly progress toward potent leads. With the implementation of an accelerated mixture synthesis workflow described in this study, we have been able to generate a mixture library within a couple of days, followed by ALIS testing and data analysis within a week. With the advantage of using label-free, soluble target protein, no extensive preparation was required prior to the binding experiments. Leveraging the capability of ALIS to analyze complex mass-encoded peptide mixtures, we

https://doi.org/10.1021/acs.jmedchem.2c00154
J. Med. Chem. 2022, 65, 8961−8974

bypassed painstaking peptide purification and only integrated one quick "clean-up" step. This accelerated Design−Make−Test cycle allowed us to explore a chemically diverse set of substitutions in a resource-sparing manner. While useful to establish the initial reliability of the ALIS competition experiments, one may not need to synthesize all individual singletons but validate only the best binders in each library and quickly deprioritize designs around weaker binders. We decided to interrogate two different adjacent positions in each of our libraries to allow for potential synergistic effects that can be difficult to uncover using single-point modifications. But any number of positions can be varied if the number of combinations and the overall physicochemical properties of the mixture library remain compatible with ALIS testing, as for instance potential solubility or aggregation issues could arise from the presence of very lipophilic peptide sequences.

In addition, in the context of intracellular targets, it is necessary to complement this binding affinity optimization with improvements in metabolic stability and cell permeability. Our results highlighted this beneficial effect of combining in peptide **7** the SAR learnings from this study with previous successful peptide stability optimization tactics to reach sustained low-micromolar cellular activity in a $KRAS^{G12D}$ pancreatic cancer cell line. With the recent clinical success against $KRAS^{G12C}$ employing covalent small molecule inhibitors exemplified by sotorasib, the search for therapeutics targeting the more common KRAS mutations like G12D and G12V has intensified. The role of peptide KRAS-binders like the KRpep-2d (**1**) series, which require polycationic peptide segments for cellular activity, remains very worthy of investigation in this regard. Keeping in mind observed off-target liabilities with such constructs, we sought to outline a path toward arginine-count reduction while maintaining cell activity, a challenging objective. Core macrocycle modifications discovered in this report offer an encouraging path forward. Further macrocycle optimization building upon the outcome of these studies to realize cell-active KRAS-inhibitory peptide scaffolds devoid of any arginine content will be the subject of upcoming communications.

EXPERIMENTAL SECTION

Chemistry. All compounds are >95% pure by HPLC, other than the ones noted in Tables S1−S6.

Peptides and Peptide Mixture Libraries were synthesized using standard solid phase synthesis using Fmoc chemistry as exemplified in the literature[41,42]

General Procedure A for Library Singletons. (A1) Solid-Phase Peptide Synthesis (SPPS). The peptide was synthesized using standard Fmoc chemistry on a 0.05 or 0.10 mmol scale using the CEM Liberty Blue automated microwave peptide synthesizer on Rink Amide MBHA LL resin (0.34 mmol/g loading). Deprotection was performed with 20% piperidine in dry DMF. Coupling reactions were performed in 5-fold excess of 0.2 M Fmoc-amino acid with 0.5 M *N,N'*-diisopropylcarbodiimide (DIC, 2 equiv to activated amino acid) ad 0.5 M Oxyma Pure (1 equiv to activated amino acid) in dry DMF (standard or double 90 °C microwave-heated coupling, 2 or 4 min). The N-terminal acetylation (capping) was performed using acetic anhydride (10% v/v in dry DMF; 75 °C for 10 min).

(A2) Cleavage and Deprotection (0.05 mmol Scale). The linear resin-bound peptide was cleaved from the solid support and deprotected by treatment with TFA/H_2O/TIS (94:3:3, v/v; 5 mL) at 41 °C for 30 min using a Razor peptide cleavage system from CEM Corporation. The resin was then filtered and rinsed with TFA (∼1 mL). The filtrates were combined and concentrated under reduced pressure to a volume of ∼2−3 mL. The crude linear peptides were precipitated from the TFA cleavage solution using cold methyl *tert*-butyl ether (MTBE; 25 mL). The suspension was cooled down on dry ice for 60 min. After centrifugation (4000 rpm, 15 min), the supernatant was discarded. The white pellet was resuspended in cold MTBE (25 mL). After cooling down on dry ice for 60 min and centrifugation (3000 rpm, 15 min), the supernatant was discarded and the white pellet was air-dried.

(A3) Cyclization and Purification (0.05 mmol Scale). The crude peptide was dissolved in acetonitrile/water (1:1, v/v; 20 mL), and 0.5 M iodine in MeOH was added until yellow color persisted. A solution of 1 M aqueous ascorbic acid was then added until a very light-yellow color persisted. Upon LC-MS confirmation of completion, the mixture was concentrated in vacuo and freeze-dried. The crude residue was then dissolved in DMSO and purified by prep-HPLC on a Waters SunFire Prep C18 OBD column (100 Å, 5 μm, column size 19 × 150 mm) using an Agilent MS-Directed Preparative HPLC/MS system. Mobile phase: (A) 0.1% TFA in HPLC water and (B) 0.1% TFA in HPLC acetonitrile; flow rate: 35 mL/min; UV wavelength λ = 215 nm. Fractions containing the desired product were combined, concentrated in vacuo, and freeze-dried to afford the cyclized peptide as a white solid.

Specific Procedure B for Mixture Libraries. (B1) Solid-Phase Peptide Synthesis (SPPS). The general procedure A1 was used for the synthesis of the mixture library except at the positions being varied where an equimolar mixture of Fmoc-protected amino acids at 0.2 M total concentration was used.

(B2) Cleavage and Deprotection. The general procedure A2 was used for the cleavage and deprotection of the peptide mixture library.

(B3) Cyclization and Purification. The crude peptide mixture was dissolved in acetonitrile/water (1:1, v/v; 20 mL), and 0.5 M iodine solution in MeOH was added dropwise until yellow color persisted. A solution of aqueous 1 M sodium ascorbate was then added until a very light-yellow color persisted. Upon LC-MS confirmation of completion, the mixture was concentrated in vacuo and freeze-dried. The crude residue was then dissolved in DMSO and semipurified by reverse-phase Teledyne ISCO flash column chromatography (FCC, RediSep Gold C18Aq 15.5 g cartridge, 30−70% gradient acetonitrile/water + 0.1% TFA over 6 column volumes). Fractions containing the desired products were combined, concentrated in vacuo, and freeze-dried to afford the desired semipurified mixture library as a white solid.

Specific Procedure C for Combination Peptides. (C1) Solid-Phase Peptide Synthesis (SPPS). The general procedure A1 was used for the solid-phase synthesis of the combination peptides.

(C2) Cleavage and Deprotection. The general procedure A2 was used for the cleavage and deprotection of the combination peptides.

(C3) Cyclization and Purification. The crude linear peptide was dissolved in acetonitrile/water (2:1, v/v; 25 mL), and DIPEA (10−20 equiv) was added to reach pH ∼9−10. DL-Dithiothreitol (DTT, 1 equiv) and diiodomethane (10 equiv) were then added, and the reaction mixture was shaken at room temperature overnight. Upon LC-MS confirmation of completion, the reaction mixture was quenched by addition of TFA (100 μL), concentrated in vacuo, and freeze-dried. The crude residue was then dissolved in DMSO and purified by prep-HPLC on a Waters SunFire Prep C18 OBD column (100 Å, 5 μm, column size 19 × 150 mm) using an Agilent MS-Directed Preparative HPLC/MS system. Mobile phase: (A) 0.1% TFA in HPLC water and (B) 0.1% TFA in HPLC acetonitrile; flow rate: 35 mL/min; UV wavelength λ = 215 nm. Fractions containing the desired product were combined, concentrated in vacuo, and freeze-dried to afford the cyclized peptide as a white solid.

SOS-Catalyzed Guanine Nucleotide Exchange (GNE) Binding Assay. The SOS-catalyzed nucleotide exchange assay utilizes a preformed complex of recombinant biotinylated KRAS protein containing G12D mutation, Bodipy-GDP, and terbium-streptavidin. Compounds are added to this complex, and then after a 60 min incubation time the mixture is treated with SOS and unlabeled GTP. Peptide inhibitors stabilize the Bodipy-GDP complex, whereas the untreated protein rapidly exchanges Bodipy-GDP for unlabeled GTP resulting in reduced TR-FRET signal.

https://doi.org/10.1021/acs.jmedchem.2c00154
J. Med. Chem. 2022, 65, 8961−8974

Biotinylated $KRAS^{G12D}$ protein is diluted to 2 mM in an EDTA buffer (20 mM HEPES pH 7.5, 50 mM sodium chloride, 10 mM EDTA, and 0.01% Tween 20) and incubated at room temperature for 1 h. This mixture is then further diluted to 90 nM in an assay buffer (20 mM HEPES pH 7.5, 150 mM sodium chloride, 10 mM magnesium chloride, and 0.005% Tween) containing 15 nM terbium-streptavidin (Invitrogen, catalog# PV3577) and 900 nM Bodipy-GDP (Invitrogen, G22360) and incubated at room temperature for 6 h. This solution is referred to as biotinylated $KRAS^{G12D}$ stock solution. For use in the final assay, the biotinylated stock solution is diluted to 1.5 nM $KRAS^{G12D}$ in assay buffer to generate the biotinylated $KRAS^{G12D}$ assay solution.

Each test compound (10 mM stock in DMSO) is diluted in DMSO to make a 10-point, 3-fold dilution series in a 384-well low dead volume microplate (Labcyte, catalog# LP-0200). Once titrations are made, 10 nL of the diluted compounds is acoustically dispensed into 384-well plates (Corning, catalog# 3820) using an Echo 550 liquid handler (Labcyte).

Each well of the assay plate receives 6 mL of Biotinylated $KRAS^{G12D}$ assay solution and is incubated at room temperature for 60 min. Each well then receives 3 mL of 120 nM recombinant human SOS protein and 9 mM GTP (Sigma, G8877) in assay buffer and is incubated at room temperature for 60 min.

The time-resolved fluorescence resonance energy transfer signal of both plates is measured on an Envision (PerkinElmer) plate reader: Excitation filter = 340 nm; emission1 = 495 nm; emission2 = 520 nm; dichroic mirror = D400/D505; delay time = 100 ms. The signal of each well is determined as the ratio of the emission at 520 nm to that at 495 nm. Percent effect of each well is determined after normalization to control wells containing DMSO (no effect) or a saturating concentration of inhibitor (max effect). The apparent effect as a function of compound concentration is fit to a four-parameter logistic equation.

Cell-Based Phospho-ERK and LDH Release Assay. AsPC-1 cells (ATCC CRL-1682TM) or A-375 cells (ATCC CRL-1619) were cultured in T175 flask with growth medium (RPMI 1640 medium, GlutaMAX Supplement, HEPES (Gibco 72400-047) or DMEM, high glucose, GlutaMAX Supplement (Gibco 10566-016) supplemented with 10% fetal bovine serum (Hyclone SH30071.03) and 1× penicillin/streptomycin (Gibco 15140-122) respectively. The cells were harvested in seeding medium (RPMI 1640 medium, no phenol red (Gibco 11835-030) or, for A-375 cells, DMEM, high glucose, no glutamine, no phenol red (Gibco 31053-028) supplemented with 10% fetal bovine serum (Hyclone SH30071.03), 25 mM HEPES (Gibco 15630−080), and 1× penicillin/streptomycin (Gibco 15140-122) after 5 min of 0.25% Trypsin-EDTA (Gibco 25200-056) digestion. AsPC-1 (A-375) cells were seeded in 384-well tissue culture treated plate (Greiner 781091) at a density of 15 000 cells (10 000 cells)/25 μL/well, and incubated at 37 °C, 5% CO_2 overnight. Prior to dosing, seeding medium was removed using the BlueCatBio Bluewasher system and replaced with 20 μL of assay medium (seeding media for respective cell lines without fetal bovine serum). The compound dose−response titrations were prepared, and appropriate amounts of compounds were dispensed into the 384-well cell culture assay plate using the Echo 550 liquid handler. Twenty-five μL of assay medium was added to achieve a final assay volume of 45 μL. The assay plate was incubated at 37 °C, 5% CO_2 for 2 and 18 h.

At 18 h post dose, 25 μL assay medium was removed and transferred to an empty 384-well tissue culture treated plate (Greiner 781091) for the LDH membrane integrity assay using the Agilent Bravo 384ST liquid handler system. For the pERK assay, remaining assay medium was removed from the plate, and cells were washed once with 25 μL 1 × DPBS (Gibco 14190-144). Cells were lysed in 20 μL of 1× lysis buffer from the AlphaScreen SureFire Ultra Multiplex pERK and total ERK assay kit (PerkinElmer MPSU-PTERK) containing EDTA-free protease inhibitor cocktail (Roche 11836170001) at ambient temperature with constant shaking at 300 rpm for 10−15 min. The cell lysates were mixed for 10 cycles using the Agilent Bravo 384ST liquid handler system before 10 μL was transferred to the OptiPlate-384 plate (PerkinElmer 6007680). Phosphorylated ERK and total ERK levels were detected with the AlphaScreen SureFire Ultra Multiplex pERK kit (PerkinElmer MPSU-PTERK) using 5 μL of acceptor bead mix and 5 μL of donor bead mix, both prepared following the manufacturer's protocol. Plates were sealed using aluminum sealing tape (Costar 07-200-683) during incubation at ambient temperature with constant shaking at 300 rpm for 1 h (both acceptor and donor). Assay plates were read on a Envision Xcite Multilabel Reader (PerkinElmer 1040900) at ambient temperature, with emission at 535 nm (total ERK) and emission at 615 nm (phospho-ERK). The ratio of pERK vs total ERK in each well was used as the final readout.

The CytoTox-ONE reaction mix was prepared from the CytoTox-ONE Homogeneous Membrane Integrity Assay Kit (Promega G7891) according to the manufacturer's protocol. Twenty-five μL of CytoTox-ONE reaction mix was added to the assay plate containing 25 μL of assay medium, and the plate was sealed using aluminum sealing tape (Costar 07-200-683). The assay plate was incubated at ambient temperature with constant shaking at 300 rpm for 45 min. Assay plates were read at ambient temperature on the Tecan M1000 instrument, with excitation at 560 nm and emission at 590 nm. Dose−response curves and EC_{50} values were analyzed using a 4-parameter logistic equation in IDBS Abase.

Cell Homogenate Stability Assay. The stability of peptides toward intracellular proteases can be evaluated using HeLa cell homogenate. Suspended HeLa cells at 1×10^6 cells/mL are sonicated in bursts with a probe sonicator on ice until they are uniformly homogenized. The homogenate thus prepared is frozen and stored at −20 °C until use. The peptides are incubated with the homogenate at 1×10^6 cells/mL, and loss of the peptide with increasing time is quantified using LC-MS/MS. The detailed protocol is available in the SI.

■ ASSOCIATED CONTENT

Supporting Information

The Supporting Information is available free of charge at https://pubs.acs.org/doi/10.1021/acs.jmedchem.2c00154.

Synthetic experimental procedures, characterization data of singleton peptides, ALIS screening procedures and data, detailed comparison of ALIS affinity ranking data sets and singletons data, SOS GNE assay, cell homogenate stability assay, AlphaScreen cellular assay, NanoClick assay, X-ray crystallography (PDF)

Molecular formula strings (CSV)

■ AUTHOR INFORMATION

Corresponding Author

Nicolas Boyer − *Merck & Co., Inc., Boston, Massachusetts 02115, United States;* orcid.org/0000-0003-1315-1660; Email: nicolas.boyer@merck.com

Authors

Michael Garrigou − *Merck & Co., Inc., Boston, Massachusetts 02115, United States*

Bérengère Sauvagnat − *Merck & Co., Inc., Boston, Massachusetts 02115, United States*

Ruchia Duggal − *Merck & Co., Inc., Boston, Massachusetts 02115, United States*

Nicole Boo − *MSD International, Singapore 138665, Singapore*

Pooja Gopal − *MSD International, Singapore 138665, Singapore*

Jennifer M. Johnston − *Merck & Co., Inc., Kenilworth, New Jersey 07033, United States;* orcid.org/0000-0003-3582-9567

Anthony Partridge − *MSD International, Singapore 138665, Singapore;* orcid.org/0000-0001-8568-2079

Tomi Sawyer − *Merck & Co., Inc., Boston, Massachusetts 02115, United States*
Kaustav Biswas − *Merck & Co., Inc., Boston, Massachusetts 02115, United States;* orcid.org/0000-0001-9971-1424

Complete contact information is available at: https://pubs.acs.org/10.1021/acs.jmedchem.2c00154

Author Contributions

The manuscript was written through contributions of all authors. All authors have given approval to the final version of the manuscript.

Notes

The authors declare no competing financial interest.

■ ACKNOWLEDGMENTS

We would like to thank Adam Beard, Mira Darlak, and Lisa Nogle for their support with peptide purification. We would like to thank Lan Ge and Andrea Peier for their support with the NanoClick assay.

■ ABBREVIATIONS

All canonical amino acids, standard one- or three-letter codes; Aad, L-α-aminoadipic acid; ACE, affinity-based competition experiment; Ahp, 2-aminoheptanoic acid; ALIS, Automated Ligand Identification System; AS-MS, affinity selection-mass spectrometry; Bip, L-4,4′-biphenylalanine; Cba, L-cyclobutylalanine; Cha, L-cyclohexylalanine; cPeA, L-cyclopentylalanine; Dab, L-2,4-diaminobutyric acid; DIC, *N,N*′-diisopropylcarbodiimide; Dip, L-diphenylalanine; DIPEA, *N,N*-diisopropylethylamine; DMEM, Dulbecco's modified Eagle's medium; DMF, *N,N*-dimethylformamide; DPBS, Dulbecco's phosphate-buffered saline; FCC, flash column chromatography; GNE, guanine nucleotide exchange; hLeu, L-homoleucine; hPhe, L-homophenylalanine; HRAS, Harvey rat sarcoma; KRAS, Kirsten rat sarcoma; LDH, lactate dehydrogenase; LL, low loading; MBHA, 4-methylbenzhydrylamine; MCD, mast cell degranulation; ND, not determined; Nle, L-norleucine; NRAS, neuroblastoma rat sarcoma; Nva, L-norvaline; OBD, optimum bed density; pERK, phosphorylated extracellular signal-regulated kinase; Phe345F3, 3,4,5-trifuoro-L-phenylalanine; PPI, protein−protein interactions; Proc4F, *cis*-4-fluoro-L-proline; Prot3OAl, *trans*-3-allyloxy-L-proline; Prot3Ph, *trans*-3-phenyl-L-proline; Prot4cHex, *trans*-4-cyclohexyl-L-proline; Prot4OAcOH, *trans*-4-(carboxymethoxy)-L-proline; PT, protein titration; RPMI, Roswell Park Memorial Institute; SEC, size exclusion chromatography; SerOMe, *O*-methyl-L-serine; SOS, son of sevenless; SPPS, solid-phase peptide synthesis; sProc35c2, *cis*-3,5-cyclopentyl-L-proline; TIS, triisopropyl silane; Tza, L-4-thiazolylalanine

■ REFERENCES

(1) Cox, A. D.; Fesik, S. W.; Kimmelman, A. C.; Luo, J.; Der, C. J. Drugging the undruggable RAS: mission possible? *Nat. Rev. Drug Discovery* **2014**, *13* (11), 828−851.
(2) Hobbs, G. A.; Der, C. J.; Rossman, K. L. RAS isoforms and mutations in cancer at a glance. *J. Cell Sci.* **2016**, *129* (7), 1287−1292.
(3) Simanshu, D. K.; Nissley, D. V.; McCormick, F. RAS proteins and their regulators in human disease. *Cell* **2017**, *170* (1), 17−33.
(4) Ostrem, J. M.; Peters, U.; Sos, M. L.; Wells, J. A.; Shokat, K. M. K-Ras(G12C) inhibitors allosterically control GTP affinity and effector interactions. *Nature* **2013**, *503* (7477), 548−551.
(5) Mullard, A. Cracking KRAS. *Nat. Rev. Drug Discovery* **2019**, *18* (12), 887−891.
(6) Papke, B.; Der, C. J. Drugging RAS: know the enemy. *Science* **2017**, *355* (6330), 1158−1163.
(7) Canon, J.; Rex, K.; Saiki, A. Y.; Mohr, C.; Cooke, K.; Bagal, D.; Gaida, K.; Holt, T.; Knutson, C. G.; Koppada, N.; Lanman, B. A.; Werner, J.; Rapaport, A. S.; San Miguel, T.; Ortiz, R.; Osgood, T.; Sun, J. R.; Zhu, X.; McCarter, J. D.; Volak, L. P.; Houk, B. E.; Fakih, M. G.; O'Neil, B. H.; Price, T. J.; Falchook, G. S.; Desai, J.; Kuo, J.; Govindan, R.; Hong, D. S.; Ouyang, W.; Henary, H.; Arvedson, T.; Cee, V. J.; Lipford, J. R. The clinical KRAS(G12C) inhibitor AMG 510 drives anti-tumour immunity. *Nature* **2019**, *575* (7781), 217−223.
(8) Fell, J. B.; Fischer, J. P.; Baer, B. R.; Blake, J. F.; Bouhana, K.; Briere, D. M.; Brown, K. D.; Burgess, L. E.; Burns, A. C.; Burkard, M. R.; Chiang, H.; Chicarelli, M. J.; Cook, A. W.; Gaudino, J. J.; Hallin, J.; Hanson, L.; Hartley, D. P.; Hicken, E. J.; Hingorani, G. P.; Hinklin, R. J.; Mejia, M. J.; Olson, P.; Otten, J. N.; Rhodes, S. P.; Rodriguez, M. E.; Savechenkov, P.; Smith, D. J.; Sudhakar, N.; Sullivan, F. X.; Tang, T. P.; Vigers, G. P.; Wollenberg, L.; Christensen, J. G.; Marx, M. A. Identification of the clinical development candidate MRTX849, a covalent KRAS(G12C) inhibitor for the treatment of cancer. *J. Med. Chem.* **2020**, *63* (13), 6679−6693.
(9) Goebel, L.; Muller, M. P.; Goody, R. S.; Rauh, D. KRasG12C inhibitors in clinical trials: a short historical perspective. *RSC Med. Chem.* **2020**, *11* (7), 760−770.
(10) First-in-Human study of JNJ-74699157 in participants with tumors harboring the KRAS G12C mutation. https://clinicaltrials.gov/ct2/show/NCT04006301 (accessed November 6, 2020).
(11) Mao, Z.; Xiao, H.; Shen, P.; Yang, Y.; Xue, J.; Yang, Y.; Shang, Y.; Zhang, L.; Li, X.; Zhang, Y.; Du, Y.; Chen, C.-C.; Guo, R.-T.; Zhang, Y. KRAS(G12D) can be targeted by potent inhibitors via formation of salt bridge. *Cell Discovery* **2022**, *8* (1), 5.
(12) Wang, X.; Allen, S.; Blake, J. F.; Bowcut, V.; Briere, D. M.; Calinisan, A.; Dahlke, J. R.; Fell, J. B.; Fischer, J. P.; Gunn, R. J.; Hallin, J.; Laguer, J.; Lawson, J. D.; Medwid, J.; Newhouse, B.; Nguyen, P.; O'Leary, J. M.; Olson, P.; Pajk, S.; Rahbaek, L.; Rodriguez, M.; Smith, C. R.; Tang, T. P.; Thomas, N. C.; Vanderpool, D.; Vigers, G. P.; Christensen, J. G.; Marx, M. A. Identification of MRTX1133, a noncovalent, potent, and selective KRASG12D inhibitor. *J. Med. Chem.* **2022**, *65* (4), 3123−3133.
(13) Pei, D.; Chen, K.; Liao, H. Targeting Ras with macromolecules. *Cold Spring Harb. Perspect. Med.* **2018**, *8* (3), a031476.
(14) Hurd, C. A.; Mott, H. R.; Owen, D. Therapeutic peptides targeting the Ras superfamily. *Pep. Sci.* **2020**, *112* (6), No. e24165.
(15) Dougherty, P. G.; Qian, Z.; Pei, D. Macrocycles as protein-protein interaction inhibitors. *Biochem. J.* **2017**, *474* (7), 1109−1125.
(16) Vinogradov, A. A.; Yin, Y.; Suga, H. Macrocyclic peptides as drug candidates: recent progress and remaining challenges. *J. Am. Chem. Soc.* **2019**, *141* (10), 4167−4181.
(17) Buyanova, M.; Cai, S.; Cooper, J.; Rhodes, C.; Salim, H.; Sahni, A.; Upadhyaya, P.; Yang, R.; Sarkar, A.; Li, N.; Wang, Q. E.; Pei, D. Discovery of a bicyclic peptidyl pan-Ras inhibitor. *J. Med. Chem.* **2021**, *64* (17), 13038−13053.
(18) Zhang, Z.; Gao, R.; Hu, Q.; Peacock, H.; Peacock, D. M.; Dai, S.; Shokat, K. M.; Suga, H. GTP-state-selective cyclic peptide ligands of K-Ras(G12D) block its interaction with Raf. *ACS Cent. Sci.* **2020**, *6* (10), 1753−1761.
(19) Sakamoto, K.; Masutani, T.; Hirokawa, T. Generation of KS-58 as the first K-Ras(G12D)-inhibitory peptide presenting anti-cancer activity in vivo. *Sci. Rep.* **2020**, *10* (1), 21671.
(20) Fumagalli, G.; Carbajo, R. J.; Nissink, J. W. M.; Tart, J.; Dou, R.; Thomas, A. P.; Spring, D. R. Targeting a novel KRAS binding site: application of one-component stapling of small (5−6-mer) peptides. *J. Med. Chem.* **2021**, *64* (23), 17287−17303.
(21) Sakamoto, K.; Kamada, Y.; Sameshima, T.; Yaguchi, M.; Niida, A.; Sasaki, S.; Miwa, M.; Ohkubo, S.; Sakamoto, J. I.; Kamaura, M.; Cho, N.; Tani, A. K-Ras(G12D)-selective inhibitory peptides generated by random peptide T7 phage display technology. *Biochem. Biophys. Res. Commun.* **2017**, *484* (3), 605−611.

(22) Niida, A.; Sasaki, S.; Yonemori, K.; Sameshima, T.; Yaguchi, M.; Asami, T.; Sakamoto, K.; Kamaura, M. Investigation of the structural requirements of K-Ras(G12D) selective inhibitory peptide KRpep-2d using alanine scans and cysteine bridging. *Bioorg. Med. Chem. Lett.* **2017**, *27* (12), 2757−2761.
(23) Sogabe, S.; Kamada, Y.; Miwa, M.; Niida, A.; Sameshima, T.; Kamaura, M.; Yonemori, K.; Sasaki, S.; Sakamoto, J. I.; Sakamoto, K. Crystal structure of a human K-Ras G12D mutant in complex with GDP and the cyclic inhibitory peptide KRpep-2d. *ACS Med. Chem. Lett.* **2017**, *8* (7), 732−736.
(24) Lim, S.; Boyer, N.; Boo, N.; Huang, C.; Venkatachalam, G.; Juang, Y.-C. A.; Garrigou, M.; Kaan, K.; Duggal, R.; Peh, K. M.; Sadruddin, A.; Gopal, P.; Yuen, T. Y.; Ng, S.; Kannan, S.; Brown, C. J.; Verma, C.; Orth, P.; Peier, A.; Ge, L.; Yu, X.; Bhatt, B.; Chen, F.; Wang, E.; Li, N. J.; Gonzalez, R. J.; Stoeck, A.; Henry, B.; Sawyer, T. K.; Lane, D. P.; Johannes, C. W.; Biswas, K.; Partridge, A. W. Discovery of cell active macrocyclic peptides with on-target inhibition of KRAS signaling. *Chem. Sci.* **2021**, *12* (48), 15975−15987.
(25) Dunayevskiy, Y. M.; Lai, J. J.; Quinn, C.; Talley, F.; Vouros, P. Mass spectrometric identification of ligands selected from combinatorial libraries using gel filtration. *Rapid Commun. Mass Sp.* **1997**, *11* (11), 1178−1184.
(26) Muckenschnabel, I.; Falchetto, R.; Mayr, L. M.; Filipuzzi, I. SpeedScreen: label-free liquid chromatography-mass spectrometry-based high-throughput screening for the discovery of orphan protein ligands. *Anal. Biochem.* **2004**, *324* (2), 241−249.
(27) Annis, D. A.; Nickbarg, E.; Yang, X.; Ziebell, M. R.; Whitehurst, C. E. Affinity selection-mass spectrometry screening techniques for small molecule drug discovery. *Curr. Opin. Chem. Biol.* **2007**, *11* (5), 518−526.
(28) Annis, D. A.; Athanasopoulos, J.; Curran, P. J.; Felsch, J. S.; Kalghatgi, K.; Lee, W. H.; Nash, H. M.; Orminati, J. P. A.; Rosner, K. E.; Shipps, G. W.; Thaddupathy, G. R. A.; Tyler, A. N.; Vilenchik, L.; Wagner, C. R.; Wintner, E. A. An affinity selection-mass spectrometry method for the identification of small molecule ligands from self-encoded combinatorial libraries - Discovery of a novel antagonist of E-coli dihydrofolate reductase. *Int. J. Mass Spectrom.* **2004**, *238* (2), 77−83.
(29) Deng, Y.; Shipps, G. W., Jr.; Cooper, A.; English, J. M.; Annis, D. A.; Carr, D.; Nan, Y.; Wang, T.; Zhu, H. Y.; Chuang, C. C.; Dayananth, P.; Hruza, A. W.; Xiao, L.; Jin, W.; Kirschmeier, P.; Windsor, W. T.; Samatar, A. A. Discovery of novel, dual mechanism ERK inhibitors by affinity selection screening of an inactive kinase. *J. Med. Chem.* **2014**, *57* (21), 8817−8826.
(30) Zhang, T.; Liu, Y.; Yang, X.; Martin, G. E.; Yao, H.; Shang, J.; Bugianesi, R. M.; Ellsworth, K. P.; Sonatore, L. M.; Nizner, P.; Sherer, E. C.; Hill, S. E.; Knemeyer, I. W.; Geissler, W. M.; Dandliker, P. J.; Helmy, R.; Wood, H. B. Definitive metabolite identification coupled with Automated Ligand Identification System (ALIS) technology: a novel approach to uncover structure-activity relationships and guide drug design in a Factor IXa inhibitor program. *J. Med. Chem.* **2016**, *59* (5), 1818−1829.
(31) Gesmundo, N. J.; Sauvagnat, B.; Curran, P. J.; Richards, M. P.; Andrews, C. L.; Dandliker, P. J.; Cernak, T. Nanoscale synthesis and affinity ranking. *Nature* **2018**, *557* (7704), 228−232.
(32) Rizvi, N. F.; Nickbarg, E. B. RNA-ALIS: methodology for screening soluble RNAs as small molecule targets using ALIS affinity-selection mass spectrometry. *Methods* **2019**, *167*, 28−38.
(33) Zuckermann, R. N.; Kerr, J. M.; Siani, M. A.; Banville, S. C.; Santi, D. V. Identification of highest-affinity ligands by affinity selection from equimolar peptide mixtures generated by robotic synthesis. *Proc. Natl. Acad. Sci. U.S.A.* **1992**, *89* (10), 4505−4509.
(34) Huyer, G.; Kelly, J.; Moffat, J.; Zamboni, R.; Jia, Z. C.; Gresser, M. J.; Ramachandran, C. Affinity selection from peptide libraries to determine substrate specificity of protein tyrosine phosphatases. *Anal. Biochem.* **1998**, *258* (1), 19−30.
(35) Touti, F.; Gates, Z. P.; Bandyopadhyay, A.; Lautrette, G.; Pentelute, B. L. In-solution enrichment identifies peptide inhibitors of protein−protein interactions. *Nat. Chem. Biol.* **2019**, *15* (4), 410−418.
(36) Tjoeng, F. S.; Towery, D. S.; Bulock, J. W.; Whipple, D. E.; Fok, K. F.; Williams, M. H.; Zupec, M. E.; Adams, S. P. Multiple peptide synthesis using a single support (MPS3). *Int. J. Pept. Protein Res.* **1990**, *35* (2), 141−146.
(37) Rutter, W. J.; Santi, D. V. General method for producing and selecting peptides with specific properties. WO8910931A1, 1989.
(38) Annis, D. A.; Nazef, N.; Chuang, C. C.; Scott, M. P.; Nash, H. M. A general technique to rank protein-ligand binding affinities and determine allosteric versus direct binding site competition in compound mixtures. *J. Am. Chem. Soc.* **2004**, *126* (47), 15495−15503.
(39) *Molecular Operating Environment (MOE)*, ver. 2020.09; Chemical Computing Group ULC: Montreal, 2022.
(40) Peier, A.; Ge, L.; Boyer, N.; Frost, J.; Duggal, R.; Biswas, K.; Edmondson, S.; Hermes, J. D.; Yan, L.; Zimprich, C.; Sadruddin, A.; Kristal Kaan, H. Y.; Chandramohan, A.; Brown, C. J.; Thean, D.; Lee, X. E.; Yuen, T. Y.; Ferrer-Gago, F. J.; Johannes, C. W.; Lane, D. P.; Sherborne, B.; Corona, C.; Robers, M. B.; Sawyer, T. K.; Partridge, A. W. NanoClick: a high throughput, target-agnostic peptide cell permeability assay. *ACS Chem. Biol.* **2021**, *16* (2), 293−309.
(41) Chan, W. C.; White, P. D. *Fmoc solid phase peptide synthesis: a practical approach*; Oxford University Press: Oxford, 2000.
(42) Benoiton, N. L. *Chemistry of peptide synthesis*; CRC Press: Boca Raton, FL, 2006.

https://doi.org/10.1021/acs.jmedchem.2c00154
J. Med. Chem. 2022, 65, 8961−8974